Assessment of drug transporters involved in the urinary secretion of [99mTc]dimercaptosuccinic acid

Masato Kobayashi [a,*,1], Asuka Mizutani [a], Takaki Okamoto [b], Yuka Muranaka [b], Kodai Nishi [c], Ryuichi Nishii [d,1], Naoto Shikano [e], Takeo Nakanishi [f], Ikumi Tamai [g], Eugenie S. Kleinerman [h], Keiichi Kawai [a,i]

a School of Health Sciences, Institute of Medical, Pharmaceutical and Health Sciences, Kanazawa University, Kanazawa, Japan
b Division of Health Sciences, Graduate School of Medical Sciences, Kanazawa University, Kanazawa, Japan
c Department of Radioisotope Medicine, Atomic Bomb Disease Institute, Nagasaki University, Nagasaki, Japan
d Department of Molecular Imaging and Theranostics, National Institute of Radiological Sciences, National Institutes for Quantum and Radiological Science and Technology, Chiba, Japan
e Department of Radiological Sciences, Ibaraki Prefectural University of Health Sciences, Ibaraki, Japan
f Faculty of Pharmacy, Takasaki University of Health and Welfare, Takasaki, Japan
g School of Pharmaceutical Sciences, Institute of Medical, Pharmaceutical and Health Sciences, Kanazawa University, Kanazawa, Japan
h Division of Pediatrics, University of Texas M.D. Anderson Cancer Center, Houston, USA
i Biomedical Imaging Research Center, University of Fukui, Fukui, Japan

ARTICLE INFO

ABSTRACT

Introduction: We clarified the renal uptake and urinary secretion mechanism of [99mTc]dimercaptosuccinic acid ([99mTc]DMSA) via drug transporters in renal proximal tubules.
Methods: [99mTc]DMSA was added to human embryonic kidney 293 cells expressing human multidrug and toxin extrusion (MATE)1 and MATE2-K, carnitine/organic cation transporter (OCTN)1 and OCTN2, and organic cation transporter (OCT)2; to Flp293 cells expressing human organic anion transporter (OAT)1 and OAT3; and to vesicles expressing P-glycoprotein (P-gp), multidrug resistance associated protein (MRP)2, MRP4, or breast cancer resistance protein with and without probenecid (OAT inhibitor for both OATs and MRPs). Time activity curves of [99mTc]DMSA with and without probenecid were established using LLC-PK1 cells. Biodistribution and single photon emission computed tomography (SPECT) imaging in mice were conducted using [99mTc]DMSA with and without probenecid.
Results: [99mTc]DMSA uptake was significantly higher in Flp293/OAT3 than in mock cells. Uptake via OAT3 was inhibited by probenecid. [99mTc]DMSA uptake into vesicles that highly expressed MRP2 was significantly higher in adenosine triphosphate (ATP) than in adenosine monophosphate (AMP), and probenecid decreased uptake to similar levels as that in AMP. In the time activity curves for [99mTc]DMSA in LLC-PK1 cells, probenecid loading inhibited accumulation from the basolateral side into LLC-PK1 cells, whereas accumulation from the apical side into cells gradually increased. Transport of [99mTc]DMSA from both sides was low. Biodistribution and SPECT imaging studies showed that [99mTc]DMSA with probenecid loading resulted in significantly higher accumulation in blood, heart, liver, and bladder after [99mTc]DMSA injection compared with control mice. Probenecid induced significantly lower accumulation in the kidney after [99mTc]DMSA injection.
Conclusions: [99mTc]DMSA accumulates in renal proximal tubular epithelial cells from blood via OAT3 on the basolateral side, and then a small volume of [99mTc]DMSA will be excreted in urine via MRP2.
Advances in knowledge: [99mTc]DMSA accumulates via OAT3 in renal proximal tubular epithelial cells and is slightly excreted from the cells via MRP2.
Implications for patient care: [99mTc]DMSA may be useful for measuring renal transport function with OAT3 in patients.

1. Introduction

99mTc-labeled dimercaptosuccinic acid ([99mTc]DMSA), which highly accumulates in the kidney cortex [1], is a major renal cortical im-

aging agent used in the diagnosis of renal parenchymal disorders [2]. Regarding the uptake mechanism of [99mTc]DMSA, two main routes for [99mTc]DMSA in renal tubular secretion have been proposed: tubular reabsorption from the glomerular ultrafiltrate and basolateral uptake from plasma by peritubular extraction. Regarding the uptake of [99mTc]DMSA on the apical side, [99mTc]DMSA is reabsorbed by megalin/cubilin-mediated endocytosis from the glomerular ultrafiltrate [3], whereas on the basolateral side, the sodium-dependent dicarboxylate transporter

NaDC-3 (*SLC13A3*) has been implicated in the uptake of [^{99m}Tc]DMSA from peritubular capillaries into proximal tubular epithelial cells [4].

Many medicines are transported and excreted via drug transporters including solute carrier (SLC) transporters and adenosine triphosphate (ATP)-binding cassette (ABC) transporters in the kidney. Human renal cells express the following major drug transporters on the apical membrane: carnitine/organic cation transporter (OCTN)1 (*SLC22A4*), OCTN2 (*SLC22A5*), multidrug and toxin extrusion (MATE)1 (*SLC47A1*), and MATE2-K (*SLC47A2*) as SLC transporters; and P-glycoprotein (P-gp; *ABCB1*), multidrug resistance-associated protein (MRP)2 (*ABCC2*), MRP4 (*ABCC4*), and breast cancer resistance protein (BCRP, *ABCG2*) as ABC transporters [5,6]. On the other hand, the following are expressed on the basolateral membrane: organic anion transporter (OAT)1 (*SLC22A6*), OAT3 (*SLC22A8*), and organic cation transporter (OCT)2 (*SLC22A2*) as SLC transporters [5,6]. Although [^{99m}Tc]DMSA accumulates in the renal cortex, the relationship between [^{99m}Tc]DMSA and these transporters has not been established. The purpose of this study is to clarify renal uptake and the urinary secretion mechanism of [^{99m}Tc]DMSA via these SLC and ABC transporters in renal proximal tubules.

2. Materials and methods

2.1. Materials

[^{99m}Tc]DMSA was produced using a labeling kit purchased from FUJIFILM Toyama Chemical Co., Ltd. (Tokyo, Japan) and ^{99m}TcO$_4^-$ eluted from a ^{99}Mo - ^{99m}Tc generator (Nihon Medi-physics Co. Ltd., Chiba, Japan). Radiochemical purity of [^{99m}Tc]DMSA was more than 95%. [^{3}H] methyl-4-phenylpyridinium was purchased from American Radiolabeled Chemicals Inc. (St. Louis, MO, USA, 2.96 TBq/mmol), and *p*-[^{14}C]aminohippuric acid was purchased from PerkinElmer Inc. (Waltham, MA, USA, 2.04 GBq/mmol). Probenecid was purchased from Sigma-Aldrich (St. Louis, MO, USA).

2.2. Human embryonic kidney (HEK)293 and Flp293 cells for SLC transporters and vesicles for ABC transporters

To investigate SLC transporters, HEK293 cells expressing OCTN1, OCTN2, MATE1, MATE2-K, and OCT2 and Flp293 cells (derived from HEK293 cells that stably express the human α_{1A}-adrenoreceptor) expressing OAT1, OAT3, or the OAT3 plasmid vector alone for mock cells were prepared as described previously [7]. Briefly, HEK293 and Flp293 cells were transfected with the respective plasmid DNA and then selected with the appropriate antibiotics; HEK293/OCTN1, HEK293/OCTN2, HEK293/MATE1, HEK293/MATE2-K, HEK293/OCT2, Flp293/OAT1, Flp293/OAT3, and mock cells were established. All cell lines were grown in Dulbecco's modified Eagle's medium (Wako Pure Chemical Industries Ltd., Osaka, Japan) supplemented with 10% (v/v) fetal bovine serum (Life Technologies, Carlsbad, CA, USA), 100 U/ml penicillin, and 100 μg/ml streptomycin at 37 °C in 5% CO$_2$.

To investigate ABC transporters, vesicles (GenoMembrane Inc., Kanagawa, Japan) that express high levels of human P-gp, MRP2, MRP4, and BCRP were used. Experimental kits were also purchased from GenoMembrane Inc. and used for experiments with each ABC transporter. The high quality of the kits was checked by this company.

2.3. Uptake experiments with HEK293 and Flp293 cells

Expression levels of SLC transporters were confirmed in HEK293 cells expressing OCTN, MATE, and OCT using [^{3}H]methyl-4-phenylpyridinium and Flp293 cells expressing OAT using *p*-[^{14}C] aminohippuric acid. One day before the uptake experiments, HEK293 and Flp293 cells expressing an SLC transporter were seeded at 4×10^5 cells/well in 12-well plastic plates. Cells were pre-incubated for 10 min using modified Hank's balanced salt solution (MHBS). Each cell

type was incubated with [^{99m}Tc]DMSA (37 kBq) for 5 min ($n = 4$), and cells were removed from the tissue culture plate using 0.25% trypsin-EDTA solution (Sigma-Aldrich). Then, the radioactivity of the cells was measured using a gamma counter. For protein assays of the cells, cellular protein content was measured with a bicinchoninic acid protein assay kit (Thermo Fisher Scientific Inc., Waltham, MA, USA) using bovine serum albumin as a standard. Uptake of [^{99m}Tc]DMSA in HEK293/OCTN1, HEK293/OCTN2, HEK293/MATE1, HEK293/MATE2-K, HEK293/OCT2, Flp293/OAT1, and Flp293/OAT3 cells was compared with uptake in mock HEK293 or Flp293 cells. Using assays with the OAT and MRP inhibitor, probenecid [8–10], [^{99m}Tc]DMSA with and without 1 mM probenecid in MHBS was added to HEK293 and Flp293 cells, and uptake of [^{99m}Tc]DMSA was examined in Flp293/OAT3 cells. The uptake of [^{99m}Tc]DMSA is shown as % injected dose (%ID)/g protein.

2.4. Uptake experiments with vesicles

After pre-incubation of vesicles for 10 min using reaction buffer consisting of 50 mM MOPS-Tris, 70 mM KCl, and 7.5 mM MgCl$_2$ in the kit, 37 kBq [^{99m}Tc]DMSA was added for 5 min to each vesicle solution that included ATP ($n = 4$), which supplies energy for ABC transporters, or adenosine monophosphate (AMP, n = 4), which does not provide energy and was used for comparison to ATP. Radioactivity of vesicles on nitrocellulose filters was measured using a γ-ray counter (AccuFLEXγ7000, Aloka, Tokyo, Japan). Uptake of [^{99m}Tc]DMSA in ATP solution was compared with that in AMP solution. A higher uptake of [^{99m}Tc]DMSA in ATP solution than in AMP solution indicated an effect of [^{99m}Tc]DMSA on ABC transporters. [^{99m}Tc]DMSA with and without 1 mM probenecid in MHBS was added to each vesicle solution. The uptake of [^{99m}Tc]DMSA is shown as %ID/mg protein.

2.5. Transport assays with LLC-PK$_1$ cells

LLC-PK$_1$ cells were cultured in Dulbecco's modified Eagle's medium (Sigma-Aldrich) supplemented with L-glutamine (2 mmol/l) and 10% fetal bovine serum without antibiotics in an atmosphere of 5.0% CO$_2$/ 95.0% air at 37 °C (pH 7.4). For preparation of a cell monolayer on a micropore support, the cells were seeded at a density of 5×10^5 cells/cm^2 on a polycarbonate membrane filter (growth surface area: 1.12 cm^2, membrane pore size: 3 μm) in Transwell cell chambers. The volumes of medium inside and outside the Transwell chamber were approximately 0.5 and 1.5 ml, respectively.

Transport assays with LLC-PK$_1$ cells were performed as described [11]. After 10-min preincubation with MHBS, [^{99m}Tc]DMSA was added to the cells ($n = 4$) with incubation medium on the apical or basolateral side. For inhibition assays, a final concentration of 1 mM probenecid [12] was added in MHBS with [^{99m}Tc]DMSA addition. For transport measurements, an aliquot (50 μl) of the incubation medium from the opposite side of the cells to which [^{99m}Tc]DMSA had been added was obtained at 5, 15, 30, 60, and 120 min after the injection start of [^{99m}Tc]DMSA incubation. At the end of the incubation, each well was rapidly washed twice with 1 ml of ice-cold incubation medium. The cells were then solubilized in 0.5 ml 0.1 N NaOH, and radioactivity was measured using an auto-well gamma counter (AccuFLEX ARC-7010, Hitachi, Hitachi, Japan). The uptake of [^{99m}Tc]DMSA is shown as %ID/mg protein.

2.6. Biological distribution of [^{99m}Tc]DMSA

All applicable institutional guidelines for the care and use of animals at Kanazawa University were followed. All procedures performed in studies involving animals were in accordance with the ethical standards of Kanazawa University (the Animal Care Committee of Kanazawa University, AP-122339) and were conducted in accordance with the international standards for animal welfare and institutional guidelines. Twenty-four ddy mice (male, 6 weeks old, SLC Inc., Hamamatsu, Japan) were housed for approximately 5–7 weeks in a 12-h light/12-h

dark cycle with free access to food and water. The mice were fasted with no food overnight with water supplied ad libitum before experiments. Then, [99mTc]DMSA (37.3 ± 0.6 kBq) was injected into mice via the tail vein. Mice with a clip on the penis to prevent urination were sacrificed at 5, 30, 60, and 120 min post-injection (n = 3 each time point). After blood was sampled via cardiocentesis, the heart, liver, kidney, and bladder were excised. Radioactivity in weighed tissue samples was measured using a gamma counter. Data are expressed as % injected dose per g wet tissue (%ID/g tissue). For the loading study with probenecid, which has a high safety level in humans, ddy mice were injected with a mixture of [99mTc]DMSA and probenecid (114.1 μg/kg mouse body weight in 100 μl saline [10,12]), and the distribution studies were performed using the same protocol that was used for ddy mice without probenecid loading as control mice.

2.7. Single photon emission computed tomography (SPECT) imaging with [99mTc]DMSA

[99mTc]DMSA (60.8 ± 3.1 MBq, n = 3) or a mixture of [99mTc]DMSA and probenecid (114.1 μg/kg mouse body weight in 100 μl saline [10,12], n = 3) was injected into the tail vein of ddy mice. SPECT acquisition was started 5 min after injection, and SPECT images were obtained at 5–10 min and 60–65 min using a U-SPECT-II/CT system (MILabs, Utrecht, The Netherlands). The data were reconstructed using the ordered subset expectation maximization method with 16 subsets and six iterations, including no scatter and attenuation correction. The voxel size was set to $0.8 \times 0.8 \times 0.8$ mm^3. Post-reconstruction smoothing filtering was applied using a 1.0-mm Gaussian filter. Image displays were obtained using medical image data analysis software, Pmod (ver.

3.7, PMOD Technologies LLC, Zurich, Switzerland). Coronal and sagittal images are displayed as similar section images.

2.8. Statistical analysis

Data are presented as means and standard deviation. After normality testing using the Kolmogorov-Smirnov test, P values were calculated using the two-tailed paired Student's t-test for comparison between two groups or analysis of variance and Dunnett's test, which were used as a multiplex analysis with a population mean value, using GraphPad Prism 7 statistical software (GraphPad Software, Inc., La Jolla, CA, USA). A P value less than 0.01 or 0.05 was considered significant.

3. Results

Before experiments with [99mTc]DMSA, we confirmed the function of SLC transporters in HEK293 and Flp293 cells using ^{3}H- or ^{14}C-labeled substrates. Uptake of [99mTc]DMSA by HEK293 and Flp293 cells expressing an SLC transporter is shown in Fig. 1. [99mTc]DMSA uptake was significantly higher in Flp293/OAT3 cells than in mock cells. Probenecid loading decreased the uptake of [99mTc]DMSA in Flp293/OAT3 cells to similar levels as that in mock cells.

Fig. 2 shows the uptake of [99mTc]DMSA by vesicles overexpressing each ABC transporter. [99mTc]DMSA uptake into vesicles that highly expressed MRP2 in the presence of ATP was significantly higher than that in the presence of AMP. Vesicles expressing MRP4, P-gp, and BCRP did not show different levels of [99mTc]DMSA uptake in ATP, AMP, or the presence of probenecid. Probenecid loading in the vesicle
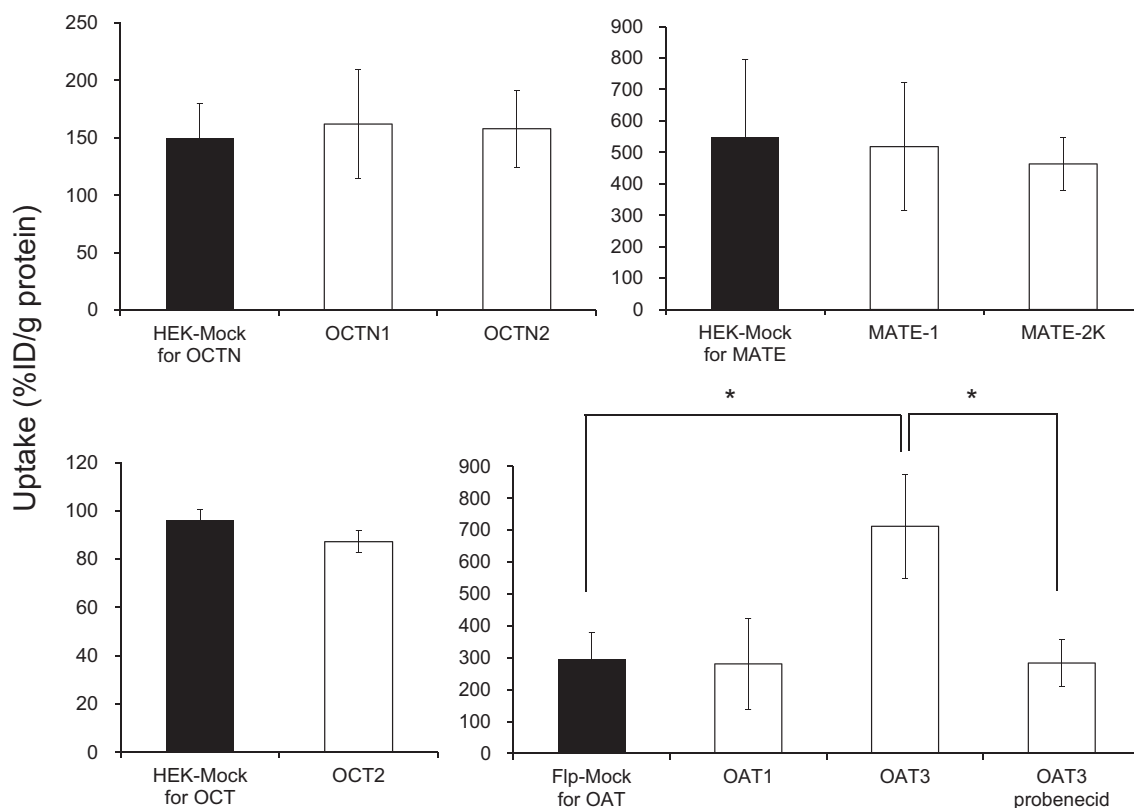
Fig. 1. Uptake of [99mTc]DMSA by HEK293 or Flp293 cells expressing a SLC transporter (n = 4). Before experiments with [99mTc]DMSA, we confirmed the function of SLC transporters in HEK293 and Flp293 cells using ^{3}H- or ^{14}C-labeled substrates. Uptake of the ^{3}H- or ^{14}C-labeled substrates into HEK293 or Flp293 mock cells as control cells was 112.3 ± 35.3%ID/g protein for HEK-Mock cells for OCTN, 318.2 ± 96.2%ID/g protein for HEK-Mock cells for MATE, 66.2 ± 15.2%ID/g protein for HEK-Mock cells for OCT, and 224.2 ± 85.0%ID/g protein for Flp-Mock cells for OAT. On the other hand, uptake of the ^{3}H- or ^{14}C-labeled substrates into HEK293 or Flp293 cells expressing a SLC transporter was as follows: 427 ± 48.4%ID/g protein for HEK293-OCTN1, 387 ± 43.7%ID/g protein for HEK293-OCTN2, 935 ± 84.9%ID/g protein for HEK293-MATE-1, 1194 ± 123.1%ID/g protein for HEK293-MATE-2 K, 592 ± 61.1%ID/g protein for HEK293-OCT2, 501 ± 62.1%ID/g protein for Flp293-OAT1, and 803 ± 98.8%ID/g protein for Flp293-OAT3. [99mTc]DMSA uptake was significantly higher in Flp293/OAT3 cells than in mock cells, and was inhibited by probenecid. *P < 0.01 vs. mock cells and HEK293 cells with probenecid loading.
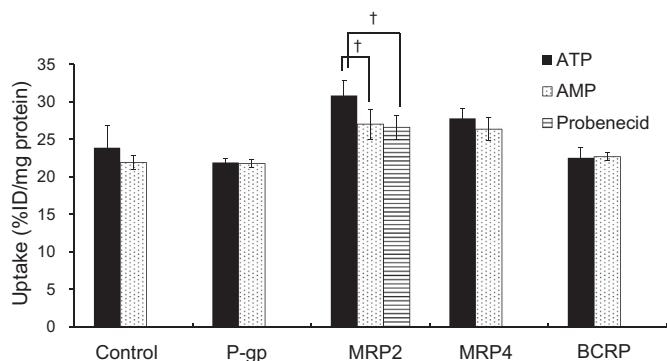
Fig. 2. Uptake of [^{99m}Tc]DMSA by vesicles overexpressing each ABC transporter ($n = 4$). [^{99m}Tc]DMSA uptake into vesicles that highly expressed MRP2 in the presence of ATP was significantly higher than that in the presence of AMP. Vesicles expressing MRP4, P-gp, and BCRP did not show different levels of [^{99m}Tc]DMSA uptake in ATP, AMP, or the presence of probenecid. With probenecid loading, uptake of [^{99m}Tc]DMSA was decreased to levels similar to that in AMP solution. $^{†}P < 0.05$ vs. the presence of AMP and ATP with probenecid loading.

solution of vesicles with high expression of MRP2 in the presence of ATP solution decreased the uptake of [^{99m}Tc]DMSA to similar levels as that in AMP solution.

In the time activity curves of [^{99m}Tc]DMSA in LLC-PK$_1$ cells (Fig. 3), accumulation from the basolateral side into LLC-PK$_1$ cells was the highest and significantly different than other conditions. Probenecid loading significantly inhibited the accumulation. On the other hand, accumulation from the apical side into cells gradually increased, and was not inhibited by probenecid. Although transport from both sides was low, transport from the apical side to the basolateral side was slightly higher than that from the basolateral side to the apical side.

The biological distribution (Table 1) and SPECT images (Fig. 4) of mice injected using [^{99m}Tc]DMSA with or without probenecid loading were obtained. Regarding the biological distribution of [^{99m}Tc]DMSA in normal mice (Table 1), [^{99m}Tc]DMSA maximally accumulated in the blood, lung, heart, liver, and muscle at 5 min and in kidney at 60 min, and then was washed out. The accumulation in bladder gradually increased. [^{99m}Tc]DMSA with probenecid loading resulted in significantly higher accumulation in the blood, heart, and liver at 5 min and bladder at 5 and 30 min after [^{99m}Tc]DMSA injection in comparison with mice not treated with probenecid. On the other hand, probenecid induced significantly lower accumulation in kidney over 5 min after [^{99m}Tc]DMSA injection. At 5 min after [^{99m}Tc]DMSA injection, the average

ratios of accumulation in kidney to blood with and without probenecid loading were 0.41 and 0.82, respectively. At 5 min, the liver-to-blood ratios with and without probenecid loading were 0.65 and 0.75, respectively. At 60 min, the average ratios of accumulation in kidney to blood with and without probenecid loading were 3.53 and 5.21, respectively, and the liver-to-blood ratios with and without probenecid loading were 0.69 and 0.75, respectively. SPECT images at 5–10 min and 60–65 min after [^{99m}Tc]DMSA (Fig. 4) showed that accumulation of [^{99m}Tc]DMSA at 5–10 min was 2.9 ± 0.8 and 1.3 ± 0.7 in the heart, 2.5 ± 0.5 and 3.2 ± 0.7 in the kidney, and 6.4 ± 2.2 and 5.0 ± 1.9%ID/g weight in the bladder with and without probenecid loading, respectively. The average ratios of accumulation in kidney to heart with and without probenecid loading were 0.86 and 2.46, respectively. At 60–65 min after [^{99m}Tc]DMSA injection, [^{99m}Tc]DMSA showed accumulation of 1.6 ± 0.5 and 1.4 ± 0.6 in the heart, 2.1 ± 0.8 and 3.7 ± 0.9 in the kidney, and 8.1 ± 3.1 and 7.4 ± 2.7%ID/g weight in the bladder with and without probenecid loading, respectively. The average ratios of accumulation in kidney to heart with and without probenecid loading were 1.31 and 2.64, respectively.

4. Discussion

In this study, accumulation and the uptake mechanism of [^{99m}Tc]DMSA via drug transporters in renal tubular epithelial cells were evaluated. [^{99m}Tc]DMSA accumulates via OAT3 from the blood into renal tubular epithelial cells on the renal basolateral side (Fig. 1), and will then be excreted into urine via MRP2 from the epithelial cells (Fig. 2). Anion drugs are usually transported by OATs, which are SLC transporters, and MRPs, which are ABC transporters, in the cells [13]. Probenecid, an inhibitor of OATs and MRPs [12], inhibited uptake of [^{99m}Tc]DMSA into Flp293/OAT3 cells and vesicles that expressed MRP2 (Figs. 1 and 2). In our previous study [14], not only technetium-99 m-labeled mercaptoacetylglycylglycylglycine ([^{99m}Tc]MAG3) but also [^{99m}Tc]DMSA had very high affinity (90% binding for [^{99m}Tc]MAG3 and 93% binding for [^{99m}Tc]DMSA) for plasma proteins at a typical clinical dose. In general, medicines with high affinity for plasma proteins in blood are transported from the blood through the renal basolateral side and excreted into urine. Therefore, we estimate that [^{99m}Tc]DMSA accumulates in the cells via SLC transporters on the renal basolateral side via OAT3.

In LLC-PK$_1$ cells, we confirmed that [^{99m}Tc]DMSA accumulated from the basolateral side into the cells and that the accumulation was inhibited by probenecid (Fig. 3a). Therefore, we confirmed that [^{99m}Tc]DMSA is transported via OAT3 on the basolateral membrane. Be-

(a)

(b)
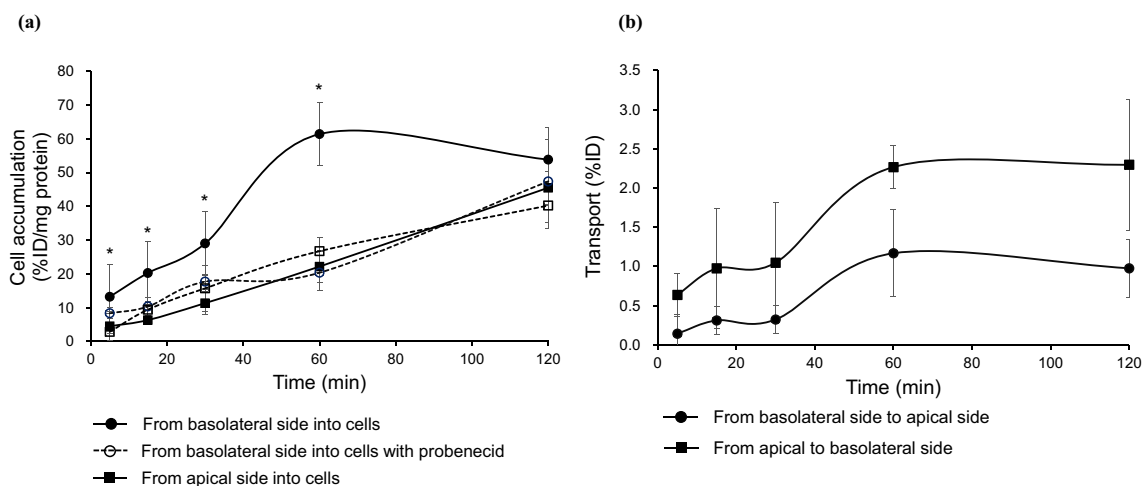
Fig. 3. Time activity curves of cell accumulation (a) and transport (b) for [^{99m}Tc]DMSA in LLC-PK$_1$ cells (n = 4). Accumulation from the basolateral side into LLC-PK$_1$ cells was significantly higher than that with probenecid loading. From the apical side into cells, the accumulation gradually increased, but probenecid did not affect accumulation. Transport from both sides was relatively low. $^{*}P < 0.01$ vs. control and probenecid loading.

Table 1
Biological distribution of [99mTc]DMSA in mice with and without probenecid loading.

|	Organ (%ID/g)	5 min	30 min	60 min	120 min
Normal mice	Blood	1.40 ± 0.21	1.01 ± 0.15	0.87 ± 0.12	0.22 ± 0.03
	Lung	0.80 ± 0.16	0.68 ± 0.15	0.61 ± 0.14	0.54 ± 0.13
	Heart	1.98 ± 0.44	1.14 ± 0.35	1.01 ± 0.25	0.42 ± 0.05
	Liver	1.05 ± 0.18	0.97 ± 0.23	0.65 ± 0.18	0.11 ± 0.03
	Kidney	1.15 ± 0.25	2.08 ± 0.39	4.53 ± 1.03	3.81 ± 0.71
	Bladder	9.82 ± 2.49	10.55 ± 3.78	12.48 ± 3.42	14.38 ± 4.39
	Muscle	0.42 ± 0.08	0.31 ± 0.07	0.22 ± 0.04	0.14 ± 0.04
Probenecid loading	Blood	1.89 ± 0.29*	1.22 ± 0.31	0.91 ± 0.22	0.28 ± 0.19
	Lung	0.83 ± 0.15	0.70 ± 0.16	0.65 ± 0.15	0.55 ± 0.14
	Heart	2.25 ± 0.41†	1.28 ± 0.43	1.09 ± 0.15	0.48 ± 0.08
	Liver	1.22 ± 0.16†	0.91 ± 0.33	0.63 ± 0.18	0.12 ± 0.04
	Kidney	0.78 ± 0.27*	1.52 ± 0.28*	3.21 ± 0.42*	2.97 ± 0.98†
	Bladder	11.91 ± 3.11†	13.17 ± 4.52†	14.71 ± 5.56	16.81 ± 7.06
	Muscle	0.44 ± 0.09	0.38 ± 0.08	0.28 ± 0.10	0.16 ± 0.09

%ID/g indicates percent injected dose per gram of tissue. Values are the means ± standard deviation obtained from three mice.
*$P < 0.01$ and †$P < 0.05$ compared with normal mice.

cause MRP2 transports medicines from the epithelial cells into the urine on the apical side in only one direction [5,6], [99mTc]DMSA was also likely to be excreted via MRP2 from the epithelial cells into the urine on the apical side. However, accumulation of [99mTc]DMSA in cells through the basolateral membrane was not increased by inhibition of MRP2 with probenecid loading because probenecid is an OAT inhibitor on the basolateral membrane and may mainly be effective on the basolateral side where probenecid was injected. Non-radioisotope-labeled DMSA also has affinity for MRP2 [15]. However, we estimate that the affinity of [99mTc]DMSA for MRP2 is lower than that of [99mTc]MAG3 for ABC transporters including MRP2 [13] because transport from the basolateral side to the apical side was low in LLC-PK1 cells (Fig. 3b). Thus, [99mTc]DMSA accumulates via OAT3 from the blood on the basolateral side into proximal tubular epithelial cells, and then some volume of [99mTc]DMSA will be excreted from the cells into the apical side via MRP2. Regarding other uptake mechanisms of [99mTc]DMSA into epithelial cells, [99mTc]DMSA is reabsorbed by megalin/cubilin-mediated endocytosis from the apical side into epithelial cells

[3] and secreted via the sodium-dependent dicarboxylate transporter NaDC-3 from peritubular capillaries on the basolateral side into proximal tubular epithelial cells [4]. Including the results of our study, because three mechanisms function for [99mTc]DMSA uptake into proximal tubular epithelial cells, most injected [99mTc]DMSA will accumulate in the cells.

Regarding the biological distribution in mice with and without probenecid loading (Table 1), [99mTc]DMSA with probenecid loading provided significantly higher accumulation in the blood, heart, liver, and bladder at 5 min after injection, whereas lower accumulation was seen in the kidney over 5 min after injection in comparison with mice without probenecid injection. Higher accumulation of [99mTc]DMSA in the bladder in the presence of probenecid was due to increased radioactivity of [99mTc]DMSA in blood, and then [99mTc]DMSA will be excreted into urine by glomerular ultrafiltration. In addition, the average ratios of accumulation in kidney or liver to blood with probenecid loading were lower than those without probenecid at early and late [99mTc]DMSA injection times.
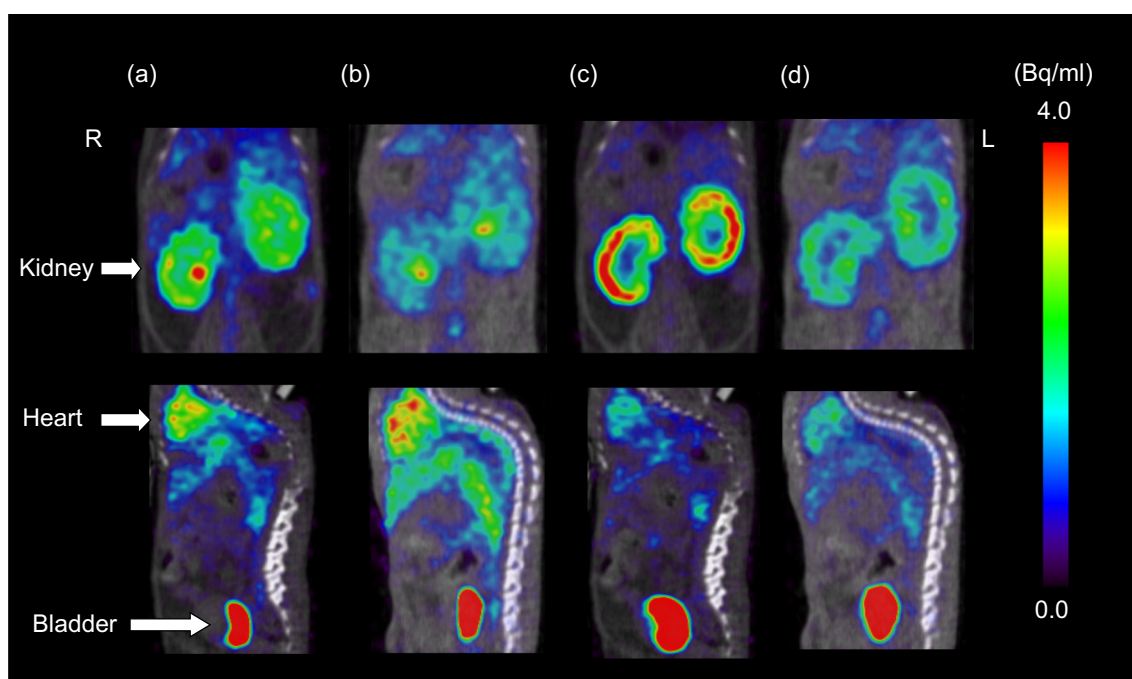
Fig. 4. Representative [99mTc]DMSA SPECT imaging without (a, c) and with (b, d) probenecid loading at 5–10 min (a, b) and 60–65 min (c, d) after injection of approximately 60 MBq [99mTc]DMSA. Probenecid, an OAT inhibitor, inhibited the accumulation of [99mTc]DMSA in kidney at 5–10 min and 60–65 min after injection under isoflurane anesthesia, whereas increased accumulation was shown in the heart at 5–10 min after injection.

On SPECT imaging using [^{99m}Tc]DMSA with probenecid loading at 5–10 min and 60–65 min after injection, accumulation of [^{99m}Tc] DMSA was significantly increased by probenecid in the heart at 5–10 min after injection, and was decreased in the kidney at 5–10 min and 60–65 min after injection (Fig. 4). SPECT imaging showed that OAT3 is involved in [^{99m}Tc]DMSA uptake from the blood into proximal tubular epithelial cells on the basolateral side as well. Similarly, the biodistribution results showed that the average ratios of accumulation in kidney to heart with probenecid loading were lower than those without probenecid at early and late [^{99m}Tc]DMSA injection times.

According to our in vitro study, [^{99m}Tc]DMSA likely accumulates via OAT3 from the blood on the basolateral side into proximal tubular epithelial cells (Fig. 1 and 3a). [^{99m}Tc]DMSA has low affinity for MRP2 (Fig. 2). In the in vivo study, we also confirmed that the uptake mechanism of [^{99m}Tc]DMSA involves OAT3 because accumulation of [^{99m}Tc] DMSA in the kidney was lower in the presence of probenecid compared with the absence. Yee et al. showed no significant difference in [^{99m}Tc] DMSA uptake in control vs. probenecid-treated rats [16]. They injected probenecid into rats at 1 h before [^{99m}Tc]DMSA injection. With [^{99m}Tc] DMSA experiments, probenecid has little effect because the competitive inhibition effect of probenecid was provided at about 30 min in our in vivo experiments. In their study, probenecid could not play a significant role in renal uptake of [^{99m}Tc]DMSA. Although rodents and humans express OAT3 [5,6] and MRP2 [17] in kidney, assessment of the expression levels of renal transporters including OAT3 and MRP2 may be important to emphasize the uptake mechanism of [^{99m}Tc]DMSA via renal transporters.

5. Conclusion

[^{99m}Tc]DMSA accumulates from the blood into renal proximal tubular epithelial cells via OAT3 on the basolateral side, and then a small volume of [^{99m}Tc]DMSA will be excreted via MRP2 in urine.

Declaration of competing interest

There is no conflict of interest.

Acknowledgments

Financial support

References

[1] Willis KW, Martinez DA, Hedley-Whyte ET, Davis MA, Judy PF, Treves S. Renal localization of ^{99m}Tc-stannous glucophetonate and ^{99m}Tc-stannous dimercaptosuccinate in the rat by frozen section autoradiography: the efficiency and resolution of technetium-99m. Radiat Res. 1977;69:475–88.
[2] Durand E, Prigent A. The basics of renal imaging and function studies. Q J Nucl Med. 2002;46:249–67.
[3] Weyer K, Nielsen R, Petersen SV, Christensen EI, Rehling M, Birn H. Renal uptake of ^{99m}Tc-dimercaptosuccinic acid is dependent on normal proximal tubule receptor-mediated endocytosis. J Nucl Med. 2013;54(1):159–65.
[4] Burckhardt BC, Drinkuth B, Menzel C, König A, Steffgen J, Wright SH, et al. The renal Na(1)-dependent dicarboxylate transporter, NaDC-3, translocates dimethyl- and disulfhydryl-compounds and contributes to renal heavy metal detoxification. J Am Soc Nephrol. 2002;13:2628–38.
[5] Ivanyuk A, Livio F, Biollaz J, Buclin T. Renal drug transporters and drug interactions. Clin Pharmacokinet. 2017;56:825–92.
[6] Yang X, Han L. Roles of renal drug transporter in drug disposition and renal toxicity. Adv Exp Med Biol. 2019;1141:341–60.
[7] Kobayashi M, Mizutani A, Nishi K, Muranaka Y, Nishii R, Shikano N, et al. [^{131}I]MIBG exports via MRP transporters and inhibition of the MRP transporters improves accumulation of [^{131}I]MIBG in neuroblastoma. Nucl Med Biol 2020;90–91:49–54.
[8] Reid G, Wielinga P, Zelcer N, De Haas M, Van Deemter L, Wijnholds J, et al. Characterization of the transport of nucleoside analog drugs by the human multidrug resistance proteins MRP4 and MRP5. Mol Pharmacol. 2003;63:1094–103.
[9] Luna-Tortós C, Fedrowitz M, Löscher W. Evaluation of transport of common antiepileptic drugs by human multidrug resistance-associated proteins (MRP1, 2 and 5) that are overexpressed in pharmacoresistant epilepsy. Neuropharmacology. 2010;58:1019–32.
[10] Takahara N, Saga T, Inubushi M, Kusuhara H, Seki C, Ito S, et al. Drugs interacting with organic anion transporter-1 affect uptake of Tc-99m-mercaptoacetyl-triglycine (MAG3) in the human kidney: therapeutic drug interaction in Tc-99m-MAG3 diagnosis of renal function and possible application of Tc-99m-MAG3 for drug development. Nucl Med Biol. 2013;40:643–50.
[11] Kobayashi M, Shikano N, Nishii R, Kiyono Y, Araki H, Nishi K, et al. Comparison of the transcellular transport of FDG and D-glucose by the kidney epithelial cell line, LLC-PK$_1$. Nucl Med Commun. 2010;31:141–6.
[12] Kobayashi M, Nishi K, Mizutani A, Okudaira H, Nakanishi T, Shikano N, et al. Transport mechanism and affinity of [^{99m}Tc]Tc-mercaptoacetyltriglycine ([^{99m}Tc]MAG3) on the apical membrane of renal proximal tubule cells. Nucl Med Biol 2020;84–85: 33–7.
[13] Kobayashi M, Tsujiuchi T, Okui Y, Mizutani A, Nishi K, Nakanishi T, et al. Different efflux transporter affinity and metabolism of ^{99m}Tc-2-methoxyisobutylisonitrile and ^{99m}Tc-tetrofosmin for multidrug resistance monitoring in cancer. Pharm Res. 2019; 36:18.
[14] Nishi K, Kobayashi M, Nishii R, Shikano N, Takamura N, Kuga N, et al. Pharmacokinetic alteration of ^{99m}Tc-MAG$_3$ using serum protein binding displacement method. Nucl Med Biol. 2013;40:366–70.
[15] Bridges CC, Joshee L, Zalups RK. Multidrug resistance proteins and the renal elimination of inorganic mercury mediated by 2,3-dimercaptopropane-1-sulfonic acid and meso-2,3-dimercaptosuccinic acid. J Pharmacol Exp Ther. 2008;324:383–90.
[16] Yee CA, Lee HB, Blaufox MD. Tc-99m DMSA renal uptake: influence of biochemical and physiologic factors. J Nucl Med. 1981;22:1054–8.
[17] Goh LB, Spears KJ, Yao D, Ayrton A, Morgan P, Wolf CR, et al. Endogenous drug transporters in in vitro and in vivo models for the prediction of drug disposition in man. Biochem Pharmacol. 2002;64(11):1569–78.